

## Supporting Information

### *In situ* bulk magnetization measurements reveal the state of charge of redox flow batteries

Evan Wenbo Zhao,<sup>a, b</sup> Edward J. K. Shellard,<sup>a</sup> Peter A. A. Klusener,<sup>c</sup> and Clare P. Grey <sup>a\*</sup>

- a. Department of Chemistry, Lensfield Road, University of Cambridge, Cambridge CB2 1EW, UK.
- b. Magnetic Resonance Research Centre, Institute for Molecules and Materials, Radboud University Nijmegen, 6525 AJ, Nijmegen, NL.
- c. Shell Global Solutions International B.V., Shell Technology Centre Amsterdam, Grasweg 31, 1031 HW Amsterdam, NL.

## Contents

|  |    |
|--|----|
| <b>Experiments</b> .....   | 4  |
| <i>In situ</i> NMR.....  | 4  |
| <i>In situ</i> bulk magnetization measurement .....  | 4  |
| <b>Calculations</b> .....  | 5  |
| Bulk magnetic susceptibility and concentration of paramagnetic species .....                                     | 5  |
| Evans balance readings calibration .....   | 5  |
| Battery capacity conversion to concentration of paramagnetic species .....                                       | 6  |
| Analytic modelling of the SOC .....  | 6  |
| <b>Supplementary figures</b> .....   | 7  |
| Fig. S1  <i>In situ</i> <sup>1</sup> H NMR spectra acquired during electrochemical cycling. ....                 | 7  |
| Fig. S2  SOC of electrolyte solution in the tank and in the flow coming out of the<br>electrochemical cell. .... | 7  |
| Fig. S3  Setup for the <i>in situ</i> bulk magnetic susceptibility measurement. ....                             | 8  |
| Fig. S4  Calibration of the Evans balance readings .....   | 9  |
| Fig. S5   Battery cycling readings from the Evans balance I. ....  | 10 |
| Fig. S6   Battery cycling readings from the Evans balance II.....  | 12 |
| <b>References</b> .....  | 13 |

## Experiments

### *In situ* NMR

The setup consists of a flow battery (Scribner), two peristaltic pumps (MasterFlex L/S 07751-20, Cole-Parmer), an electrochemical cycler (SP-150, BioLogic SAS), and an NMR (300 MHz, Bruker) spectrometer. Details of the NMR sampling tube are provided in our previous publication and are shown in Fig. 1.<sup>1,2</sup> In the battery, 20 cm<sup>3</sup> of 200 mM K<sub>4</sub>[Fe(CN)<sub>6</sub>] was used as the catholyte and 20 cm<sup>3</sup> of 300 mM 2,6-dihydroxyanthraquinone (AQ) was used as the anolyte. The solvent was D<sub>2</sub>O with 1 M KOH as the supporting electrolyte for the catholyte, and 1.6 M KOH for the anolyte. The battery comprises of two graphite flow plates with serpentine flow patterns, two 4.6 mm carbon felt electrodes (SGL) with a 5 cm<sup>2</sup> active area and a Nafion 212 membrane. The carbon felt electrodes were used as received without further treatment and were compressed by 2.2% ((4.6 mm – 4.5 mm)/4.6 mm) in the battery. The Nafion 212 membrane was treated by first heating the membrane in deionized water at 80 °C for 20 min and then soaking it in 5% hydrogen peroxide solution at room temperature for 35 min. The treated membrane was stored in 0.1 M KOH solution at room temperature for at least 24 hours before usage. The flow rate of the electrolytes was set at 13.6 cm<sup>3</sup>/min. Pseudo-2D NMR experiments were performed by direct excitation with a 90° radio-frequency pulse. Each NMR spectrum was acquired by collecting 8 free induction decays with a recycle delay of 5 s. The pulse width for a 90° pulse was 27 μs. All spectra were referenced to the water chemical shift at 4.79 ppm before battery cycling was started.

### *In situ* bulk magnetization measurement

To measure the magnetic susceptibility, we used an Evans balance (Johnson-Matthey, Mark I) and modified a 3 mm NMR tube to act as an electrolyte reservoir and be placed in the balance at a depth of 50 mm (see Fig. S3 for details of the setup). The readings on the Evans balance were recorded by two cameras (this particular model of this balance not providing any digital output). Our initial analysis reported here, measured the magnetic susceptibility every 5 minutes using five data points, each separated by 10 s, which were used to give an average and calculate the standard deviation, as represented by the error bars in the graph. In the battery, 15 cm<sup>3</sup> of 500 mM K<sub>3</sub>[Fe(CN)<sub>6</sub>] was used as the catholyte. 15 cm<sup>3</sup> of 300 mM AQ was used as the anolyte. The solvent was H<sub>2</sub>O with 1 M KOH as the supporting electrolyte for the catholyte, and 1.6 M KOH for the anolyte. The flow rates for both electrolyte solutions were set at 7.3 cm<sup>3</sup>/min. The battery setup used a pre-treated Nafion 212 membrane and 3x sheets of carbon paper (without further treatment) as electrodes.

A calibration of the Evans balance measurements was carried out using the same set up and flow rate with prepared concentrations of K<sub>3</sub>[Fe(CN)<sub>6</sub>] varying between 0 M and 0.5 M. A linear graph was then drawn up correlating the balance readings with the known concentration (Fig. S4). The Evans balance readings could then be correlated directly to magnetic susceptibility  $\Delta\chi$  using Eqs. S1 and S8.

## Calculations

### Bulk magnetic susceptibility and concentration of paramagnetic species

The NMR chemical shift of water  $\Delta\delta$ , is caused by the change of bulk magnetic susceptibility (BMS) of the electrolyte,  $\Delta\chi$ , following the well-established relationship.<sup>4</sup>

$$\Delta\delta = \frac{4}{3}\pi\Delta\chi \quad \#(S1)$$

Here,  $\Delta\chi$  is related to the change of concentration of the paramagnetic species,  $\Delta C_P$ , by

$$\Delta\chi = \frac{N_A \mu_{eff}^2 \mu_B^2}{3k_B T} \Delta C_P \quad \#(S2)$$

where  $N_A$  is Avogadro's constant,  $k_B$  is the Boltzmann constant,  $T$  is temperature in Kelvin,  $\mu_B$  is the Bohr magneton, and  $\mu_{eff}$  is the effective magnetic moment in units of Bohr magnetons (BM). Eq. S2 is in CGS unit. Assuming the spin-only formula, valid when the contributions to the orbital angular momentum can be ignored (and spin-orbit coupling is quenched or inherently zero),  $\mu_{eff}$  is a direct measure of the number of unpaired electrons,  $n$ :

$$\mu_{eff} = \sqrt{n(n+2)} \quad \#(S3)$$

where  $n$  can also be written in terms of  $S$  the total quantum spin number of the system ( $S = n/2$ ).

Combining Eqs. S1 and S2, we obtain,

$$\Delta C_P = \frac{9 k_B T}{4\pi N_A \mu_{eff}^2 \mu_B^2} \Delta\delta \quad \#(S4)$$

where  $\Delta C_P$  is linearly related to  $\Delta\delta$ . The shift  $\Delta\delta$  can be obtained from the NMR spectra.  $\Delta C_P$  can be calculated from the current during the electrochemical cycling, following

$$Q = N_A q_e v \Delta C_P \quad \#(S5)$$

where  $Q$  is the capacity of the battery,  $q_e$  is the charge of an electron ( $1.602 \times 10^{-19} C$ ),  $v$  is the volume of the electrolyte. Combining Eqs. 2 and 5, we obtain,

$$\Delta\chi = \frac{\mu_{eff}^2 \mu_B^2}{3k_B T q_e v} Q \quad \#(S6)$$

where  $\Delta\chi$  is linearly proportional to  $Q$ .  $Q$  is measured by

$$Q = It \quad \#(S7)$$

where  $I$  is the charging current and  $t$  is the charging time.

Replacing  $\mu_{eff}$  by 2.14 BM in Eq. S4, including the other constants, we obtain,

$$\Delta C_P = 122.18 \Delta\delta \quad \#(S8)$$

## Evans balance readings calibration

The Evans balance was calibrated by taking readings at different concentrations (with flow) of paramagnetic Fe(III) and plotting a linear line of best fit (Figs. S4, S5d., S6f.). Five readings were taken at each concentration to give an average and the standard deviation was used as the error. Equations S1 and S8 above were used to convert this concentration  $\Delta C_p$  to magnetic susceptibility  $\Delta\chi$  for the graphs that show both on each y axis.

## Battery capacity conversion to concentration of paramagnetic species

The capacity,  $C$ , gives how much stored charge there is in the battery, and was given in units of mA.h. First this had to be converted to units of coulombs, C.

$$1 \text{ mA.h} = 3.6 \text{ C} \#(S9)$$

The number of moles of free electrons,  $n_e$ , analogous to the number of moles of paramagnetic Fe(III) can be calculated from the charge stored in the battery by using

$$n_e = \frac{1}{N_A e} C \#(S10)$$

where  $e$  is the elementary charge and  $N_A$  is Avogadro's constant. Convert this into a concentration,  $C_p$ , using the volume,  $V$  ( $= 1.5 \times 10^{-2} \text{ dm}^3$ ), of the solution.

$$C_p = \frac{1}{V} n_e \#(S11)$$

## Analytic modelling of the SOC

A simple numerical model for a single cell RFB was made in excel to calculate the SOC in the tanks, which equals the cell inlets, and in the cell outlets. The following assumptions were made:

- tank and cell modelled as continuous stirred-tank reactor
- 100% efficiency, no side reactions
- volume of transport lines ignored
- electrolyte intake is divided over tanks and half-cells
- the time increments are maximal half of the lowest residence time in one of half-cells

## Supplementary figures

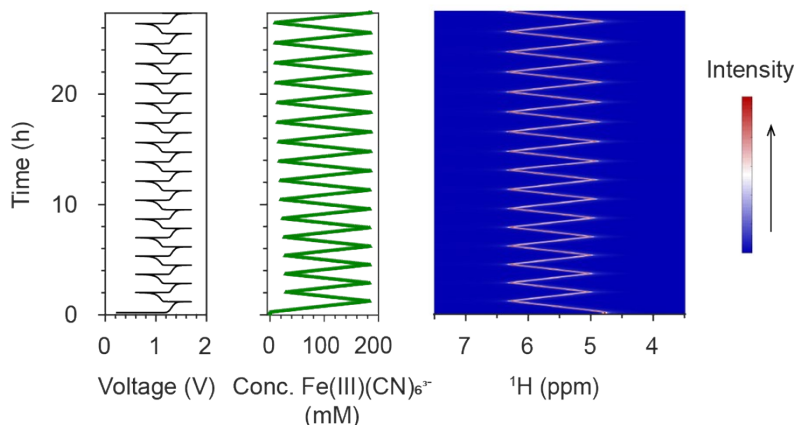


**Fig. S1 | In situ  $^1\text{H}$  NMR spectra acquired during electrochemical cycling.** The voltage, concentration and  $^1\text{H}$  NMR spectra of the catholyte obtained from a  $20\text{ cm}^3$   $200\text{ mM}$   $\text{K}_4[\text{Fe}(\text{CN})_6]$  versus  $20\text{ cm}^3$   $300\text{ mM}$  AQ full cell, acquired while charging/discharging with a current of  $100\text{ mA}$ . The colour scale indicates the intensity of the resonances in arbitrary units. The NMR signal arises from resonances of water molecules which are existing in the form of  $\text{H}_2\text{O}$  or  $\text{HDO}$ .

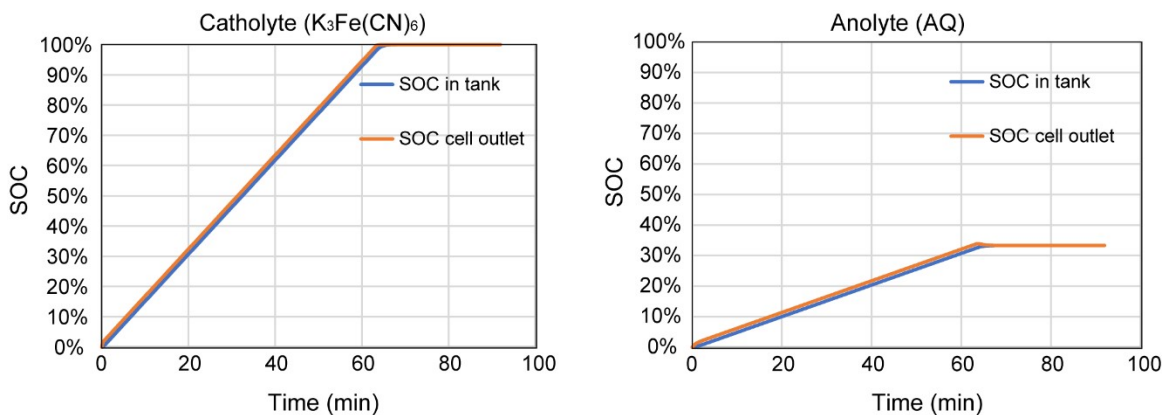


**Fig. S2 | SOC of electrolyte solution in the tank and in the flow coming out of the electrochemical cell.** The results were derived under the condition of starting with  $20\text{ cm}^3$  of  $200\text{ mM}$   $\text{K}_4[\text{Fe}(\text{CN})_6]$  as the catholyte and  $20\text{ cm}^3$  of  $300\text{ mM}$  2,6-dihydroxyanthraquinone (AQ) as the anolyte with a charging current of  $100\text{ mA}$ . The flow rate is  $13.6\text{ cm}^3/\text{min}$  and the volume of the electrolyte solution in the electrochemical half-cell is  $5\text{ cm}^3$  for both the catholyte and anolyte.

Figure S2 shows the results for the conditions as applied in the *in-situ* NMR experiment. The SOC differences between cell out- and inlet of the catholyte and the anolyte are  $1.7\%$  and  $1.4\%$ , respectively.

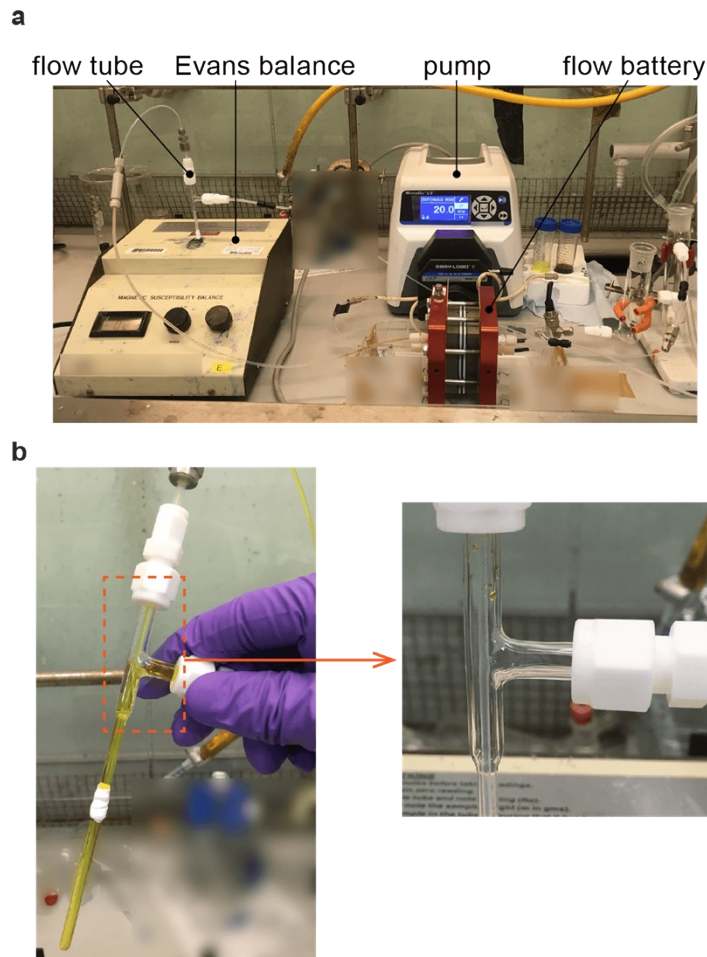


**Fig. S3 | Setup for the in situ bulk magnetic susceptibility measurement.** a. The battery is set up next to an Evans balance. One electrolyte solution is pumped through a flow sampling apparatus in the Evans balance and flowed back to the electrolyte reservoir. b. Flow sampling apparatus designed for the Evans balance. A 1/16" PFA tube is used as the inlet and inserted to the bottom of a 3 mm O.D. glass tube. The side arm on the right is the outlet. The white connectors are 1/8" to 1/4" Swagelok connectors made of TEFLON. A short piece of 1/8" PFA tube is connected to this connector and another 1/8" to 1/16" Swagelok connector (bored-through) at the top. The 1/16" PFA tube passes through these connectors and the 1/8" tube to the bottom of the glass tube. The inset on the right shows the 1/16" PFA tube inside the glass tube.

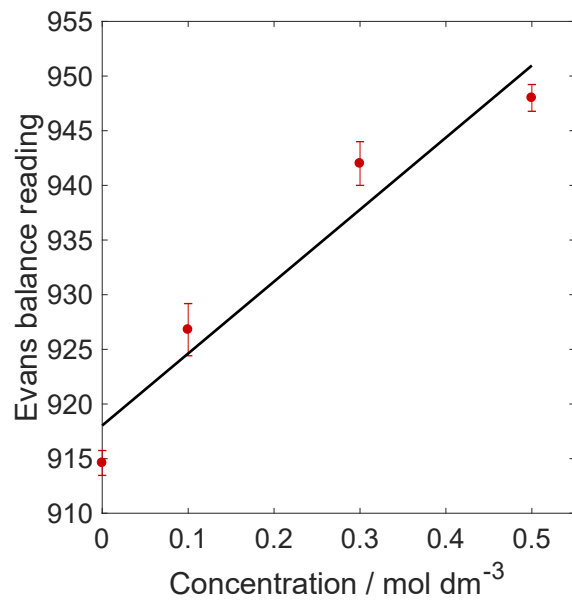


**Fig. S4 | Calibration of the Evans balance readings against standard solutions of paramagnetic  $K_3[Fe(III)(CN)_6]$ , the fitted line being used to extract the concentrations presented in the main body of the paper.**

Two additional experiments with similar parameters were carried out to explore the sensitivity of the measuring device used here to any potential interference from the local environment and the overall stability of the balance.

The first experiment used a linear charge-discharge cycle between 0.6 V and 1.7 V (Fig. S5). The flow rate was 7.7 cm<sup>3</sup>/min and pre-treated Nafion 212 membrane and 4.6mm thick carbon felt (with 2.2% compression) electrodes were used for the battery setup. This first experiment was not carried out in an adequately isolated environment and the experiment was disturbed a number of times as it was running. There is an overall downwards drift in the readings as a result, which is clearly visible when comparing with the expected concentrations calculated from the capacity (determined electrochemically). A correction to this data was applied to these readings by assuming the existence of a linear downward drift and subtracting a linearly changing offset curve from the measured experimental data. This simple correction results in a good fit to the data. The calibration curve performed at the end of the experiment (Figure S5d), again shows that the response of the instrument is linear with concentration over a short time-period, but suggests that the older Evans balance used in these measurements needs to be used in a more controlled environment and is not necessarily stable over multiple days.

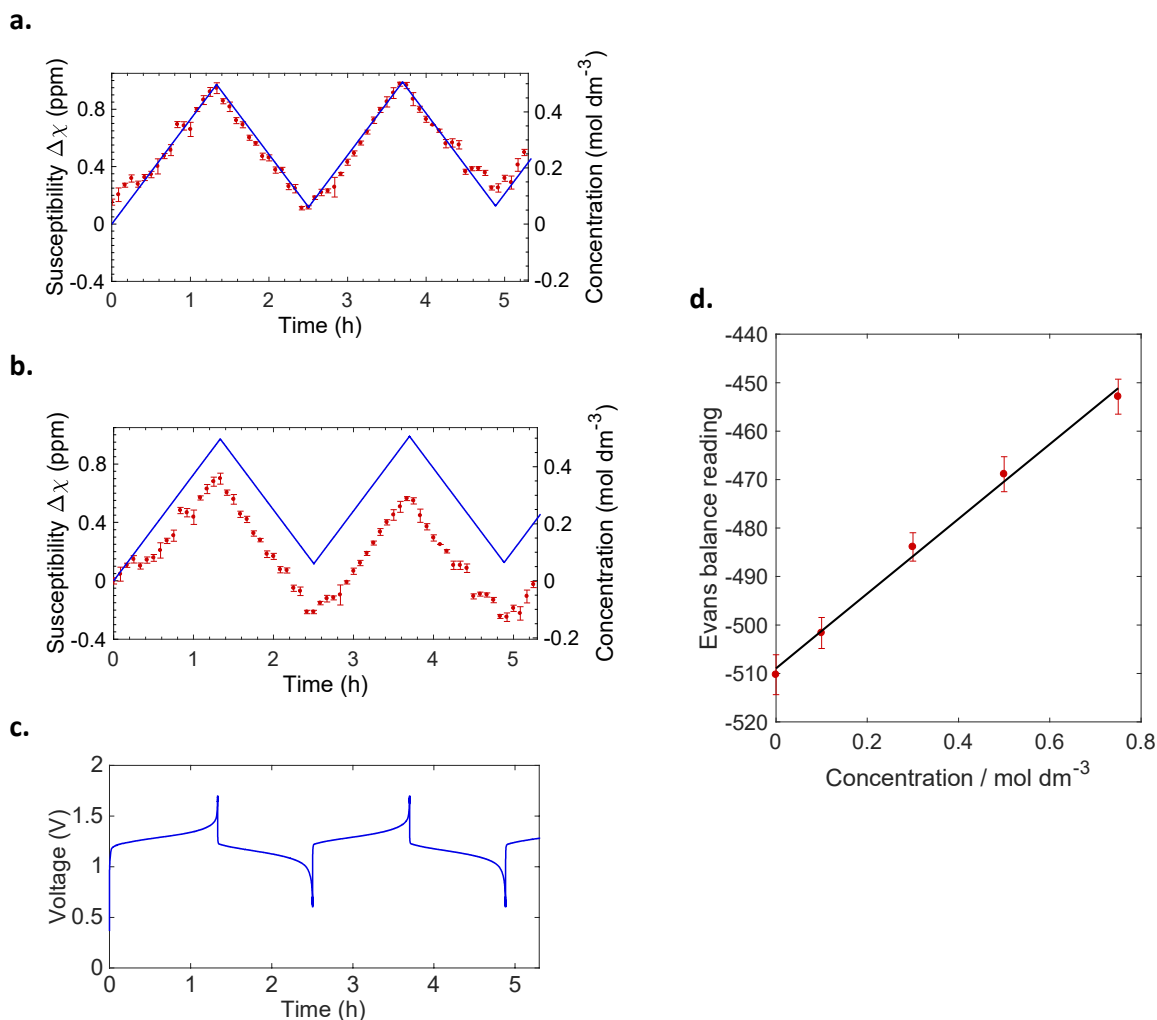


**Fig. S5 | Battery cycling readings from the Evans balance I.** a. Graph of magnetic susceptibility readings and concentration of  $[\text{Fe(III)(CN)}_6]^{3-}$  as calculated from the linear drift corrected Evans balance readings (red) and the capacity (blue). b. Graph a. but without a linear correction applied to the Evans balance readings. c. Voltage curve for the experiment. d. Calibration curve from this experiment, taken the following day after the battery was disassembled.

A second experiment (Fig. S6) was then performed with the same cycling protocol as that presented in the main body of the paper (with one hour potential holds). The battery setup here used a thicker pre-treated Nafion 117 membrane with 4.6mm thick carbon felt electrodes (with 2.2% compression) and had a flow rate of 7.7 cm<sup>3</sup>/min. Attempts were made to stabilise the environment of the experiment, but no temperature was recorded. Again, the capacity could be corrected with the same linear drift correction as used for Experiment 1. However, by 19 hours the instrument had stabilised and no correction was required. Again, the calibration curve performed at the end of the experiment was linear.

Finally, a third experiment was performed now monitoring the temperature, restricting any airflow over the instrument, minimising any movement of equipment or metal nearby, and after

the instrument had stabilised for a longer period. These results are presented in Figure 4 of the main text. This experiment does illustrate that even with the older balance used here, when the temperature changes are minimal and care is used to minimise disturbance, stable readings can be obtained even with this instrument.

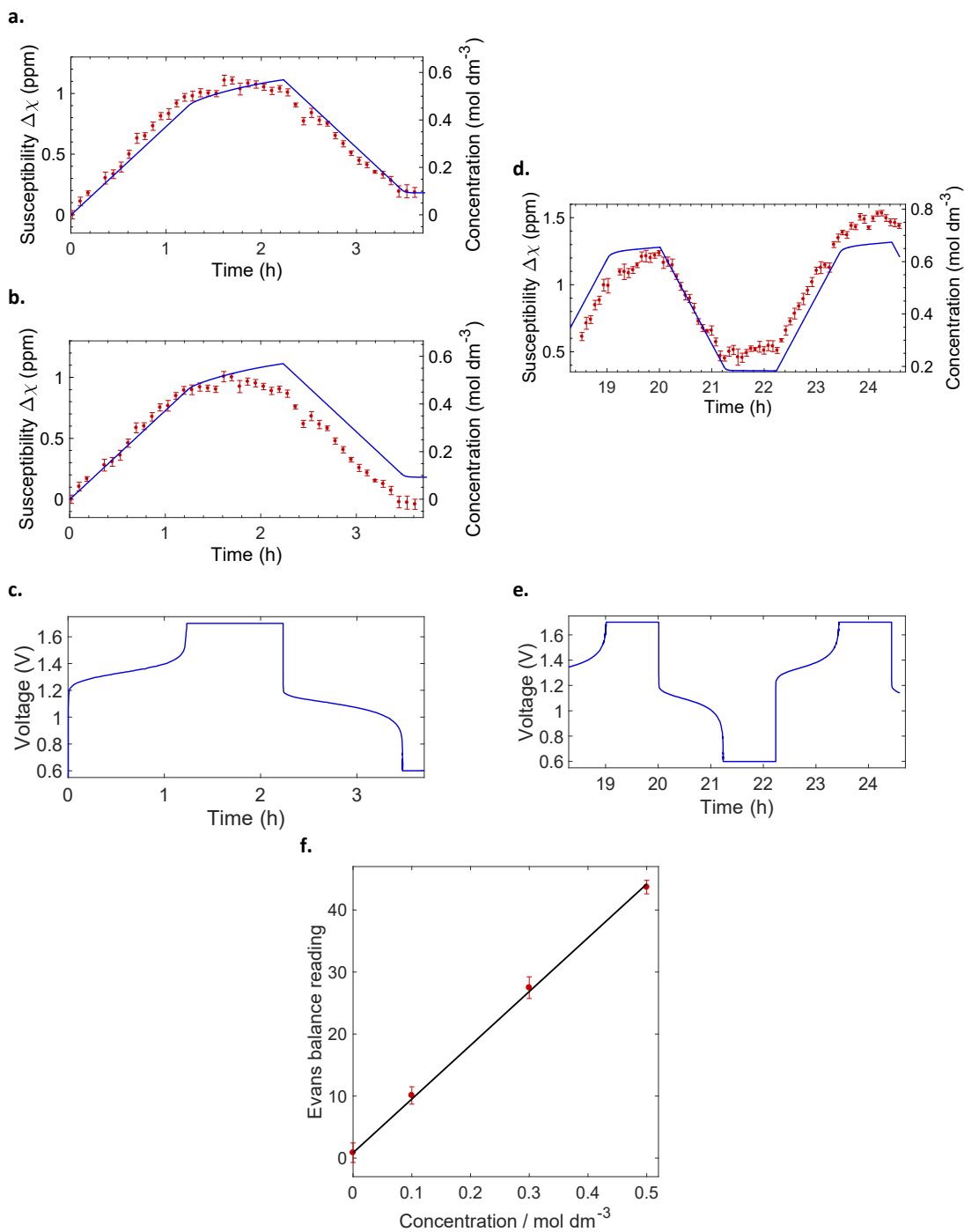


**Fig. S6 | Battery cycling readings from the Evans balance II.** a. Graph of magnetic susceptibility and concentration of [Fe(III)(CN)<sub>6</sub>]<sup>3-</sup> as calculated from the Evans balance readings (red), that have been corrected as described above, and overlaid with values as calculated from the capacity (blue) for the early part of the experiment. b. Graph shows same as a. but with uncorrected values from Evans balance readings. c. Voltage curve for the first section of the experiment. d. Graph of uncorrected magnetic susceptibility readings from the Evans balance (red), overlaid with values as calculated from the capacity (blue) for later section of experiment. e. Voltage curve for the later part of the experiment. f. Calibration of Evans balance reading with standard solutions of paramagnetic K<sub>3</sub>[Fe(CN)<sub>6</sub>].

## References

- 1 D. F. Evans, *Journal of the Chemical Society (Resumed)*, 1959, (0), 2003-2005.
- 2 E. W. Zhao, T. Liu, E. Jónsson, J. Lee, I. Temprano, R. B. Jethwa, A. Wang, H. Smith, J. Carretero-González, Q. Song and C. P. Grey, *Nature*, 2020, 579 (7798), 224-228.
- 3 Teachspin, INC (2021). Foundational Magnetic Susceptibility [Online]. Available from: <https://www.teachspin.com/fms> [Accessed 09/11/2021]
- 4 E. W. Zhao, E. Jónsson, R. B. Jethwa, D. Hey, D. Lyu, A. Brookfield, P. A. A. Klusener, D. Collison, C. P. Grey, *J. Am. Chem. Soc.* 2021, 143 (4), 1885-1895.